Chromosome breakage after G2 checkpoint release

Article (Accepted Version)

Revision of Manuscript #200612047; submitted Jan 18, 2007:

Chromosome breakage following G2 checkpoint release

Dorothee Deckbar,[1] Julie Birraux,[2] Andrea Krempler,[1] Leopoldine Tchouandong,[1] Andrea Beucher,[1] Sarah Walker,[2] Tom Stiff,[2] Penny Jeggo,[2] and Markus Löbrich[1]

[1]Fachrichtung Biophysik, Universität des Saarlandes, 66421 Homburg/Saar, Germany

[2]Genome Damage and Stability Centre, University of Sussex, East Sussex, BN1 9RQ, UK

Correspondence to Penny Jeggo: p.a.jeggo@sussex.ac.uk; or Markus Löbrich: markus.loebrich@uniklinik-saarland.de

Running head:
Chromosome breakage following G2 checkpoint release

Markus Löbrich
Saarland University
Biophysics Department
66421 Homburg/Saar
Germany
Tel. +49-6841-1626202
Fax +49-6841-1626160

20544 characters and 4 figures

Key words: Double strand break repair; Cell cycle checkpoints; Chromosome aberrations; Ataxia telangiectasia; Artemis

Abstract

DNA double-strand break (DSB) repair and checkpoint control represent distinct mechanisms to reduce chromosomal instability. Ataxia telangiectasia (A-T) cells have checkpoint arrest and DSB repair defects. Here, we examine the efficiency and interplay of ATM's G2 checkpoint and repair functions. Artemis cells manifest an identical and epistatic repair defect to A-T but show proficient checkpoint responses. Only a few G2 cells enter mitosis within 4 h following irradiation with 1 Gy but manifest multiple chromosome breaks. Most checkpoint-proficient cells arrest at the G2/M checkpoint, with the length of arrest being dependent upon the repair capacity. Strikingly, cells released from checkpoint arrest display 1-2 chromosome breaks. This represents a major contribution to chromosome breakage. The presence of chromosome breaks in cells released from checkpoint arrest suggests that release occurs prior to the completion of DSB repair. Strikingly, we show that checkpoint release occurs at a point when ~3-4 premature chromosome condensation (PCC) breaks and ~20 γH2AX foci remain.

Introduction

DNA damage response mechanisms function to maintain genomic stability in normal cells. Since genomic instability is a characteristic of cancer cells, it is evident that at least some of these damage response pathways become impaired during progression to carcinogenesis. Additionally, patients with defective damage response pathways frequently show cancer predisposition, of which ataxia telangiectasia (A-T) is a well-known example. Significant insight has been gained into the roles of individual damage response pathways. Understanding the efficiency as well as the interplay between them is an important next step (Difilippantonio et al., 2000; Gao et al., 2000).

DNA double-strand break (DSB) repair and cell cycle checkpoint arrest represent two pathways to maintain genomic stability (Wahl and Carr, 2001; van Gent et al., 2001; Lieber et al., 2003; Kruhlak et al., 2006; Bekker-Jensen et al., 2006; Mari et al., 2006). Ataxia telangiectasia mutated (ATM) plays a critical role in regulating cell cycle checkpoint arrest in response to DSBs (Shiloh, 2003; Ward and Chen, 2004; Lou et al., 2006) and also regulates a component of DSB repair (Kühne et al., 2004; Riballo et al., 2004). The prevailing evidence suggests that in G0/G1 ATM is required for Artemis, a nuclease, to process a subset (~15%) of radiation-induced DSBs prior to rejoining. A-T, a disorder caused by mutations in ATM, is associated with pronounced chromosomal instability, cancer susceptibility, and clinical radiosensitivity. This has generally been attributed to ATM's role in cell cycle checkpoint regulation. However, older cytogenetic data (Cornforth and Bedford, 1985; Jeggo et al., 1998) and the recent repair defect described in A-T cells (Riballo et al., 2004) raises the issue of how ATM's repair and checkpoint functions interplay to maintain chromosome stability. Here, we exploit A-T as a model to define the efficiency and dissect the interplay between DNA repair and cell cycle checkpoint pathways, focusing our attention on two ATM dependent functions; DSB repair in G2 and G2/M checkpoint arrest.

Results and discussion

ATM and Artemis dependent DSB repair operates in G1 and G2

To investigate the contribution of ATM and Artemis to DSB repair in cell cycle phases other than G0, we analysed asynchronously growing cell cultures to avoid the potential introduction of DSBs during synchronisation. In one approach, we used pan-nuclear centromere protein F (CENP-F) staining to identify G2 cells (Liao et al., 1995; Kao et al., 2001) (Suppl. Fig. 1A) and added aphidicolin to prevent S phase cells progressing into G2 during analysis. Mitotic cells exhibiting distinct centromeric CENP-F staining and condensed chromatin were excluded from analysis. Under these conditions, S-phase cells do not progress into G2 (Suppl. Fig. 1B) and a considerable proportion of cells irradiated with 1.5 Gy X-rays remain positive for pan-nuclear CENP-F staining for 6-8 h (ie they remain in G2), providing sufficient time to detect the ATM/Artemis repair defect which is measurable at >4 h post irradiation in G0 cells.

Enumeration of γH2AX foci in aphidicolin treated, CENP-F positive primary human fibroblasts following 1.5 Gy X-irradiation demonstrated that ATM and Artemis dependent DSB repair operates in G2 (Fig. 1A). Aphidicolin treatment did not affect the repair capacity of G2 cells (Suppl. Fig. 1C) but caused pronounced H2AX phosphorylation in cells that were CENP-F negative but positive for the S/G2 marker, CyclinA, most likely due to the activation of ATR following replication arrest (Suppl. Fig. 1A). Enumeration of γH2AX foci in CENP-F negative cells which were also negative for the pronounced, aphidicolin-induced γH2AX phosphorylation allowed the analysis of repair in G1-phase cells (Fig. 1A). For all cell lines, we observed similar kinetics and magnitude of repair in G1 and G2, which was also similar to that previously observed in G0 cells (Riballo et al., 2004). Foci numbers correlated with DNA content being twice as high in G2 compared with G1 (Fig. 1A). In analogy to our previous study (Riballo et al., 2004), we confirmed that ATM and Artemis operate in the same repair pathway by analysing the repair defect in Artemis cells treated with the specific ATM small molecule inhibitor KU55933 (Hickson et al., 2004). The dual deficiency in Artemis and ATM

did not cause an increased repair defect relative to the defect in Artemis cells (Fig. 1B). Thus, ATM and Artemis are epistatic in G1 and G2, and function to repair a subfraction of DSBs similar to that observed in confluent cells. Since our results were obtained with non-isogenic human cell lines, we also investigated γH2AX foci formation in matching wild type (WT), A-T and Artemis mouse embryonic fibroblasts (MEFs) using similar procedures to those employed with human cells and observed identical repair kinetics (Suppl. Fig. 1D).

To substantiate that γH2AX foci analysis monitors DSB repair, we developed and applied a pulsed-field gel electrophoresis (PFGE) technique to monitor DSB repair specifically in G2-phase cells (Fig. 1C). Exponentially growing primary human fibroblasts were pulse-labeled with [methyl-^{3}H]thymidine for 1 h and irradiated with 80 Gy 4 h after labeling (when in G2 (see below)). Following 48 and 72 h of repair, cells were harvested and the fraction of radioactivity released from the gel plug into the gel (the "FAR value") was quantified by liquid scintillation counting. The FAR values after repair incubation provide an estimate of the level of unrepaired DSBs and can be compared to FAR values obtained from samples analysed immediately after irradiation without repair. FACS analysis of parallel samples labeled with BrdU instead of [methyl-^{3}H]thymidine showed that labeled cells have progressed to late S/G2 at the time of irradiation (4 h after labeling) and remained in G2 for at least 72 h after irradiation with 80 Gy (Suppl. Fig. 1E). We obtained a similar level of unrepaired DSBs in A-T and Artemis cells which was similar to (or slightly higher than) the level of DSBs induced in cells irradiated with 10 Gy and not incubated for repair (ie about 1/8 of the DSBs induced by 80 Gy remain unrepaired) (Fig. 1C). Thus, the magnitude of the G2 repair defect measured by PFGE is similar to the ~15% repair defect observed by γH2AX foci analysis of G2 or G1 cells (Fig. 1A) and confluent cells (Riballo et al., 2004). The identical repair defect of A-T and Artemis cells in G2 and G1 is perhaps surprising given that ATM has been reported to be required for homologous recombination. One possible explanation is that Artemis has a role in DSB repair processes other than non-homologous end joining.

Alternatively, our findings could indicate that the majority of IR-induced DSBs are repaired by non-homologous end joining in G1 and G2. In support of this, we have observed that DNA ligase IV- and Ku80-deficient MEFs have a similar, major DSB repair defect in G1 and G2 (data not shown).

Artemis cells show normal checkpoint induction and prolonged G2/M arrest

Previously, we presented evidence that Artemis cells show normal G2/M checkpoint activation assessed by counting mitotic cells up to 9 h post ionising radiation (IR) (Riballo et al., 2004). Subsequently, Zhang et al. (2004) using phosphoH3 FACS analysis concluded that cells treated with Artemis siRNA show premature release from the G2/M checkpoint, implicating Artemis in IR-induced checkpoint responses. To examine the maintenance as well as the activation of G2/M arrest, we counted mitotic cells up to 24 h post IR in cells treated with nocodazole to accumulate cells in mitosis. We confirm that Artemis cells, in contrast to A-T cells, show normal G2/M checkpoint induction and, importantly, maintain arrested for the same length and possibly greater than WT cells (Suppl. Fig. 2A).

We next analysed the G2/M checkpoint by phosphoH3 FACS analysis and observed checkpoint activation in Artemis but not A-T cells (Fig. 2A). WT cells were released from checkpoint arrest 4-6 h after 1.3 Gy and 12 h after 6 Gy X-irradiation. Significantly, Artemis cells were released slightly later after 1.3 Gy and failed to be released for at least 16 h after 6 Gy (Fig. 2A and Suppl. Fig. 2B). Normal checkpoint induction and a prolonged arrest at the G2/M border was also observed in irradiated Artemis MEFs compared with WT MEFs (Fig. 2B). We also evaluated the time course for the progression of G2 cells through mitosis into G1 by analysing BrdU-labeled cells. Exponentially growing fibroblasts were pulse-labeled with BrdU for 1 h and irradiated with 1 Gy 4 h after labeling (when in G2). G2/M checkpoint arrest results in the retention of BrdU-labeled cells in G2. Quantification of the BrdU-labeled G2 cells for up to 12 h post irradiation confirmed that Artemis cells exhibit a prolonged G2/M

arrest (Fig. 2C). The prolonged arrest of Artemis cells in Fig. 2 was less evident in the experiments involving mitotic counting (Suppl. Fig. 2A), which may reflect the use of nocodozole in the latter approach which delays re-entry from G2/M arrest. Our observation of a prolonged arrest in Artemis cells is consistent with a role of Artemis in DSB repair in G1 and G2. One explanation for the difference between our results and those of Zhang et al. (2004) is that their study utilised human tumour cells for siRNA knock down of Artemis. Such cells frequently behave aberrantly due to abnormal levels of Chk1/Chk2 or cell cycle checkpoint regulation.

ATM's G2 checkpoint and repair functions both contribute to the avoidance of chromosome breakage

Having established that Artemis affects ATM's role in G2 DSB repair but not its function in G2 checkpoint control, we wished to evaluate the contribution of these two ATM functions to the prevention of chromosome aberrations in primary human WT, A-T and Artemis fibroblasts (Fig. 3). We focused on chromosome breaks arising from G2 irradiated cells by adding aphidicolin to prevent S-phase cells from progressing into G2 during analysis. Growing cell populations were irradiated with 1 Gy and analysed for chromosome breaks per mitotic cell at early times (2 and 4 h) post IR, similar to that undertaken in previous studies (Kemp and Jeggo, 1986). In all cell lines, chromosome breaks decreased with time reflecting DSB repair (Figs. 3A and B). A-T cells show a pronounced elevation of the number of chromosome breaks per mitotic cell (~3-fold higher than WT cells) whilst Artemis cells exhibit about two-fold more breaks/cell than WT cells consistent with Artemis' repair function in G2 (Fig. 3A). Thus, a combined checkpoint and repair defect is more severe than a repair defect alone.

We also evaluated the contribution of repair and checkpoint loss to chromosome aberration formation by utilizing the checkpoint inhibitor SB218078. This drug has been

described to impact upon Chk1 activity (Zhao et al., 2002) and abolishes 53BP1 foci formation after hydroxyurea treatment, a Chk1 dependent phenotype (Suppl. Fig. 3A) (Sengupta et al., 2004). Addition of SB218078 completely abolished the G2/M checkpoint response in primary human fibroblasts as well as in MEFs (Suppl. Fig. 3B and C) whilst repair of IR-induced DSBs in G2 remained unaffected (Suppl. Fig. 3D). SB218078 had no effect on chromosome aberration formation in A-T cells but increased the level of chromosome breaks/cell in Artemis cells to that of A-T cells (Fig. 3B). WT cells treated with SB218078 showed considerably fewer breaks/cell than drug-treated A-T or Artemis cells which represents the contribution of ATM/Artemis-dependent DSB repair to the prevention of chromosome aberrations in the absence of checkpoints. It is noteworthy that the cells forming chromosome aberrations are those in G2 at the time of irradiation as the addition of aphidicolin prevented S phase cells from progressing into G2 during analysis. Thus, any role of Chk1 in replication fork stability will not affect chromosome aberration formation. Moreover, SB218078 did not cause chromosome breaks in the absence of IR.

Cells released from the G2/M checkpoint exhibit chromosome aberrations in mitosis

Our studies predict that 1 Gy irradiated G2 phase Artemis cells would harbour 9-12 DSBs that remain unrepaired for prolonged times (see below). The release of Artemis cells from G2/M checkpoint arrest 6-8 h after irradiation suggested that the G2/M checkpoint might be unable to detect 9-12 DSBs. To investigate whether DSB repair is complete at the point of checkpoint release, we evaluated chromosome aberrations in mitotic cells that arise following checkpoint release (ie at time points greater than 4 h post IR) (Fig. 3). Since WT and Artemis cells progress from G2 into G1 within 12 h post IR with 1 Gy (see Fig. 2C), we evaluated chromosome breakage up to this time point. Strikingly, the level of chromosome aberrations in WT and Artemis cells at times when the cells that had initiated the checkpoint leave G2 (4-8 h in WT and 6-10 h in Artemis) is about 1 to 2 breaks per cell (Fig. 3A), which is more than

10-fold above the background number of chromosome breaks. Thus, almost all cells released from the G2 checkpoint exhibit chromosome aberrations in mitosis. This observation represents direct experimental evidence that the human G2/M checkpoint is not maintained until the completion of repair.

This prompted us to investigate the time course for the appearance of chromosome aberrations in mitosis. Cells entering mitosis at early times exhibit more chromosome breaks than cells entering at later times (Fig 3A). However, this analysis fails to consider the number of cells reaching mitosis at each time point. Thus, we assessed the number of cells reaching mitosis under the same conditions used for our chromosomal studies (ie in the presence of aphidicolin) by using phosphoH3 FACS analysis (Fig. 3C) and estimated the total number of mitotic chromosome breaks by multiplying the chromosome breaks per cell by the number of mitotic cells (Fig. 3D; see supplemental text for details of this estimation). Considering this novel concept, we examined the kinetics for mitotic chromosome breakage and observed a maximum at times after the G2/M checkpoint has been released (ie at 6-8 h in WT and at 8-10 h in Artemis cells). Thus, cells released from the checkpoint (at $\geq$6 h post IR) as opposed to cells which escape checkpoint arrest at early times (at $\leq$4 h post IR) represent a major cause of mitotic chromosome breakage (Fig. 3D). We also evaluated the number of cells reaching mitosis from the progression of BrdU-labeled G2 cells (obtained from Fig. 2C). An estimation of the kinetics for mitotic chromosome breakage using this analysis provided similar results to that utilizing the phosphoH3 FACS data (Suppl. Fig. 3E). Thus, the concept of evaluating chromosome breakage by considering breaks per mitotic cell as well as the number of mitotic cells reveals the striking finding that checkpoint release prior to the completion of repair represents a major cause for chromosome aberration formation. Remarkably, the total number of breaks in released cells is similar in WT and Artemis cells, although they arise with delayed kinetics in the repair defective cells. The decrease in breaks at prolonged times post treatment (>10 h) is due to the depletion of irradiated G2 cells, ie nearly all cells have left G2.

A-T cells display entirely different kinetics. Due to the lack of checkpoint arrest, they display an elevated number of chromosome breaks that decreases with time in part due to DSB repair and due to the rapid depletion of the G2 population.

The G2/M checkpoint has a defined threshold

Our findings above establish that all cells released from the G2 checkpoint harbour unrepaired damage, strongly suggesting that the G2/M checkpoint has a threshold. Our observation that Artemis cells remain checkpoint arrested longer than WT cells (Fig. 2) but are released with a similar number of γH2AX foci (Fig. 1A) or mitotic chromosome breaks (Fig. 3A) supports this notion. However, we sought other procedures to confirm the presence of DSBs in G2 at the time of checkpoint release and to evaluate the sensitivity limit of the G2 checkpoint. As one approach, we performed premature chromosome condensation (PCC) of G2 cells using the phosphatase inhibitor calyculin A (Fig. 4A). G2 cells are readily distinguished from mitotic cells and allow the analysis of PCC breaks (Asakawa and Gotoh, 1997). At 4 and 6 h post 1 Gy X-irradiation, the time at which checkpoint release commences in WT and Artemis cells respectively, we observed 3-4 PCC breaks per cell consolidating the presence of DSBs at the time of checkpoint release (Fig. 4A). Moreover, WT cells at 4 h and Artemis cells at 6 h, harbour a similar number of PCC breaks. Interestingly, these studies also provide an additional demonstration of a repair defect in Artemis cells. Previous studies equating PCC breaks with DSBs estimated by PFGE have reported a 1:3-6 relationship (ie 3-6 DSBs equate to 1 PCC break) (Cornforth and Bedford, 1993). Thus, our PCC data suggest a sensitivity level of 10-20 DSBs.

We also utilized γH2AX foci as a further marker to determine whether DSB repair is complete at the time of checkpoint release. We scored the number of foci in CENP-F positive G2-phase cells at differing times post IR and, in the same population of cells, counted the number of mitotic cells (Fig. 4B). We utilised exponentially growing transformed human

fibroblasts which provide a high mitotic index (MI). Mitotic cells were scored as phosphoH3 positive cells with condensed chromatin. Consistent with the findings above, we observed that checkpoint duration increases with dose and that cells are released from the checkpoint with ~20 foci (Fig. 4B). Similar results were obtained with hTert immortalised fibroblasts (data not shown). We also analysed mitotic cells at the 6 and 8 h time points and observed foci numbers similar to those of G2 cells demonstrating that the cells released from the checkpoint do enter mitosis with foci and that there is no selection for cells exiting the checkpoint (Suppl. Fig. 3F). Previously, we and others have observed a 1:1 relationship between γH2AX foci and DSBs (Rogakou et al., 1999; Redon et al., 2002; Rothkamm and Löbrich, 2003; Rothkamm et al., 2003). Although it is possible that γH2AX foci analysis could over-estimate DSBs remaining if repair is completed prior to the loss of visible foci, this is unlikely to occur in Artemis deficient cells, where unrepaired DSBs persist for many days in G1 and G2. Thus, our studies analysing γH2AX foci are consistent with a threshold of 10-20 DSBs. Additionally, our PFGE studies with G2 (Fig. 1C) and previously with G0 cells show that ~15% of the induced DSBs remain unrepaired in Artemis cells for many days. PFGE studies estimated 30-40 DSBs induced per Gy in G1 (Cedervall et al., 1995; Löbrich et al., 1995). Since G2 Artemis cells irradiated with 1 Gy are completely released from G2 by 12 h, the estimated persisting damage level (15% of 60-80 DSBs induced: 9-12 DSBs) is unable to maintain the checkpoint. In contrast, after 6 Gy, the level of DSBs remaining exceeds the threshold and results in arrest being maintained for at least 16 h. Hence, our PFGE data, which do not rely on γH2AX foci analysis, also indicate that the G2/M checkpoint threshold is greater than 9-12 DSBs.

To evaluate whether induction of the G2/M checkpoint has a similar sensitivity limit, we analysed transformed and immortalised fibroblasts exposed to doses up to 2 Gy at 2 h post irradiation, the earliest time point at which we observed complete arrest in pilot experiments (Fig. 4C). Cells irradiated with 0.6 Gy or higher show complete checkpoint arrest.

Significantly, the foci level 2 h after 0.6 Gy is about 20. Lower levels cause a partial arrest (Fig. 4C). Since repair occurs during the 2 h incubation necessary to measure checkpoint induction, our findings are consistent with a level of ~20 foci being required to activate checkpoint arrest. We also considered it important to examine primary human cells. The low MI of primary cells necessitated FACS analysis to estimate MI, precluding a parallel evaluation of γH2AX foci formation. Our findings were similar to those obtained using transformed/immortalised cells (Fig. 4C). Importantly, use of a lower dose inducing less than 10 γH2AX foci did not induce any detectable arrest. Based on 30-40 DSBs induced per Gy in G1, 20 DSBs are induced after doses of 0.25-0.33 Gy in G2 cells. This correlates with the mild checkpoint induction observed here after 0.2-0.3 Gy and the absence of checkpoint arrest after 0.1 Gy (Fig. 4C). Thus, these findings are consistent with a similar threshold number of DSBs (10-20) both activating and maintaining checkpoint arrest. The existence of a threshold for G2/M checkpoint arrest provides a potential explanation for low dose hypersensitivity, a phenomenon describing exquisite cellular sensitivity at low radiation doses (Marples et al., 2004). Indeed, a G2/M threshold of ~20 DSBs would predict the reported survival responses.

In conclusion, we have examined the efficacy of ATM's repair and checkpoint functions in G2, and dissected the contribution of these two ATM functions to the avoidance of chromosomal breakage. We demonstrate that (i) the kinetics of DSB repair in G2 is similar to that in G1 and that A-T and Artemis cells display an identical and epistatic repair defect in G2 as in G1; (ii) Artemis cells are G2/M checkpoint proficient; (iii) chromosome breaks occur 0-4 h post IR in a small fraction of cells that fail to arrest at the G2/M checkpoint; (iv) the majority of cells arrest at the G2/M checkpoint but give rise to 1-2 chromosome breaks upon release. This represents a major cause of chromosome aberration formation. (v) The G2/M checkpoint has a defined threshold which we estimate to be ~3-4 PCC breaks or ~10-20 DSBs. This threshold allows for the generation of 1-2 chromosome breaks in mitosis.

Materials and methods

Cell culture, chemicals, and irradiation

Cells were grown as described (Riballo et al., 2004). 10, 15 or 20 % FCS was used depending on the cell line. For the FAR assay, cells were labeled with 37 kBq/ml [methyl-^{3}H]Thymidine (2,81 TBq/mmol; Amersham) for 1 h (electrophoresis was performed according to Kühne et al. (2004)). Aphidicolin and nocodazole (Sigma) were added at 3 µg/ml and 100 ng/ml, respectively. Inhibition of Chk1 activity was achieved by addition of SB218078 (2.5 µM; Calbiochem) 30 min prior to IR. ATMi (KU55933) was added at 10 µM 30 min prior to IR. X-irradiation was performed at 90 kV or 120 kV, γ-irradiation using a ^{137}Cs- source. Dosimetry was performed with ion chambers and considered the increase in dose for cells grown on glass coverslips relative to plastic surfaces (manuscript in preparation).

Metaphase spreads and PCC

To collect metaphases, 100 ng/ml colcemid (Sigma) was added 2 h before harvesting (1 h for the 2 h time point and 4 h for the 12 h time point). For PCC analysis, cells were treated with 50 ng/ml calyculin A (Calbiochem) for 30 min before harvesting. Chromatid breaks and excess fragments (counted as 2 chromatid breaks) were scored in 20-100 chromosome spreads from at least three independent experiments per data point.

FACS

Cells pulse-labeled with 10 µM BrdU (Roche) for 1 h were analysed according to standard protocols. For phosphoH3 staining, cells were permeabilised with PBS/0.25% Triton X-100 (15 min on ice), incubated in 100 µl α-phosphoH3 antibody (Ser10) (7.5 µg/ml PBS/1% BSA) (Upstate) over night, then treated with the Alexa Fluor 488-conjugated goat-α-mouse (MoBiTec) or a FITC-conjugated swine α-rabbit antibody (DakoCytomation) in PBS/1% BSA for 1 h, followed by 50 µg/ml propidium iodide containing 0.5 mg/ml RNAse in PBS for

30 min at room temperature. Analysis was performed on a FACScan™ or FACSCalibur™ using the CellQuest software (Becton Dickinson).

Immunofluorescence

Cells grown on coverslips were fixed in 100% methanol (-20°C) for 30 min, permeabilised in acetone (-20°C) for 1 min and washed 3x10 min in PBS/1% FCS. Samples were incubated with primary antibodies (monoclonal or polyclonal α-γH2AX antibody 1:200; Upstate; polyclonal α-CENP-F and α-CyclinA antibody 1:200; Santa Cruz; or polyclonal α-phosphoH3 antibody (Ser10) 1:200, Upstate) in PBS/1% FCS for 1 h at room temperature, washed in PBS/1% FCS for 3x10 min, and incubated with Alexa Fluor 488-, Alexa Fluor 546- or Alexa Fluor 594-conjugated secondary antibodies (MoBiTec, 1:500) for 1 h at room temperature. Cells were washed in PBS for 4x10 min and mounted using Vectashield mounting medium containing 4,6 diamidino-2-phenylindole (Vector Laboratories, Burlingame, CA). In a single experiment, cell counting was performed until at least 40 cells and 40 foci were registered per sample. Each data point represents two to three independent experiments. Error bars represent the SE between the different experiments.

Acknowledgements

We thank Dr. G. Smith for providing the ATM inhibitor KU55933. The ML laboratory is supported by the Deutsche Forschungsgemeinschaft (Grant LO 677/4-1/2 and Graduiertenkolleg 377/3), the Bundesministerium für Bildung und Forschung via the Forschungszentrum Karlsruhe (Grants 02S8132 and 02S8335) and the Deutsche Zentrum für Luft und Raumfahrt e.V. (Grant 50WB0017). The PAJ laboratory is supported by the Medical Research Council, the Human Frontiers Science Programme, the Primary Immunodeficiency Association, the Leukaemia Research Fund and EU grant (FIGH-CT-200200207).

Abbreviations list

A-T, ataxia telangiectasia

ATM, ataxia telangiectasia mutated

CENP, centromere protein

DSB, double-strand break

FAR, fraction of radioactivity released

MI, mitotic index

PCC, premature chromosome condensation

PFGE, pulsed-field gel electrophoresis

MEF, mouse embryo fibroblast

WT, wild type

References

Asakawa, Y., and E. Gotoh, E. 1997. A method for detecting sister chromatid exchanges using prematurely condensed chromosomes and immunogold-silver staining. *Mutagenesis.* 12:175-177.

Bekker-Jensen, S., C. Lukas, R. Kitagawa, F. Melander, M.B. Kastan, J. Bartek, and J. Lukas. 2006. Spatial organization of the mammalian genome surveillance machinery in response to DNA strand breaks. *J. Cell Biol.* 173:195-206.

Cedervall, B., R. Wong, N. Albright, J. Dynlacht, P. Lambin, and W.C. Dewey. 1995. Methods for the quantification of DNA double-strand breaks determined from the distribution of DNA fragment sizes measured by pulsed-field gel electrophoresis. *Radiat. Res.* 143:8-16.

Cornforth, M.N., and J.S. Bedford. 1985. On the nature of a defect in cells from individuals with ataxia-telangiectasia. *Science.* 227:1589-1591.

Cornforth, M.N., and J.S. Bedford. 1993. Ionizing radiation damage and its early development in chromosomes. *Adv. Radiat. Biol.* 17:423-496.

Difilippantonio, M.J., J. Zhu, H.T. Chen, E. Meffre, M.C. Nussenzweig, E.E. Max, T. Ried, and A. Nussenzweig. 2000. DNA repair protein Ku80 suppresses chromosomal aberrations and malignant transformation. *Nature.* 404:510-514.

Gao Y., D.O. Ferguson, W. Xie, J.P. Manis, J. Sekiguchi, K.M. Frank, J. Chaudhuri, J. Horner, R.A. DePinho, and F.W. Alt. 2000. Interplay of p53 and DNA-repair protein XRCC4 in tumorigenesis, genomic stability and development. *Nature.* 404:897-900.

Hickson, I., Y. Zhao, C.J. Richardson, S.J. Green, N.M. Martin, A.I. Orr, P.M. Reaper, S.P. Jackson, N.J. Curtin, and G.C. Smith. 2004. Identification and characterization of a novel and specific inhibitor of the ataxia-telangiectasia mutated kinase ATM. *Cancer Res.* 64:9152-9159.

Jeggo, P.A., A.M. Carr, and A.R. Lehmann. 1998. Splitting the ATM: distinct repair and checkpoint defects in ataxia-telangiectasia. *Trends Genet.* 14:312-316.

Kao, G.D., W.G. McKenna, and T.J. Yen. 2001. Detection of repair activity during the DNA damage-induced G2 delay in human cancer cells. *Oncogene.* 20:3486-3496.

Kemp, L.M., and P.A. Jeggo. 1986. Radiation-induced chromosome damage in X-ray-sensitive mutants (xrs) of the Chinese hamster ovary cell line. *Mutat. Res.* 166:255-263.

Kruhlak, M.J., A. Celeste, G. Dellaire, O. Fernandez-Capetillo, W.G. Muller, J.G. McNally, D.P. Bazett-Jones, and A. Nussenzweig. 2006. Changes in chromatin structure and mobility in living cells at sites of DNA double-strand breaks. *J. Cell Biol.* 172:823-834.

Kühne, M., E. Riballo, N. Rief, K. Rothkamm, P.A. Jeggo, and M. Löbrich. 2004. A double-strand break repair defect in ATM-deficient cells contributes to radiosensitivity. *Cancer Res.* 64:500-508.

Liao, H., R.J. Winkfein, G. Mack, J.B. Rattner, and T.J. Yen. 1995. CENP-F is a protein of the nuclear matrix that assembles onto kinetochores at late G2 and is rapidly degraded after mitosis. *J. Cell Biol.* 130:507-518.

Lieber, M.R., Y. Ma, U. Pannicke, and K. Schwarz. 2003. Mechanism and regulation of human non-homologous DNA end-joining. *Nat. Rev. Mol. Cell Biol.* 4:712-720.

Löbrich, M., B. Rydberg, and P.K. Cooper. 1995. Repair of x-ray-induced DNA double-strand breaks in specific Not I restriction fragments in human fibroblasts: joining of correct and incorrect ends. *Proc. Natl. Acad. Sci. USA.* 92:12050-12054.

Lou, Z., K. Minter-Dykhouse, S. Franco, M. Gostissa, M.A. Rivera, A. Celeste, J.P. Manis, J. van Deursen, A. Nussenzweig, T.T. Paull, F.W. Alt, and J. Chen. 2006. MDC1 maintains genomic stability by participating in the amplification of ATM-dependent DNA damage signals. *Mol. Cell.* 21:187-200.

Mari, P.O., B.I. Florea, S.P. Persengiev, N.S. Verkaik, H.T. Bruggenwirth, M. Modesti, G. Giglia-Mari, K. Bezstarosti, J.A. Demmers, T.M. Luider, A.B. Houtsmuller, and D.C. van

Gent. 2006. Dynamic assembly of end-joining complexes requires interaction between Ku70/80 and XRCC4. *Proc. Natl. Acad. Sci. USA.* 103:18597-18602.

Marples, B., B.G. Wouters, S.J. Collis, A.J. Chalmers, and M.C. Joiner. 2004. Low-dose hyper-radiosensitivity: a consequence of ineffective cell cycle arrest of radiation-damaged G2-phase cells. *Radiat Res.* 161:247-255.

Redon, C., D. Pilch, E. Rogakou, O. Sedelnikova, K. Newrock, and W. Bonner. 2002. Histone H2A variants H2AX and H2AZ. *Curr. Opin. Genet. Dev.* 12:162-169.

Riballo, E., M. Kühne, N. Rief, A. Doherty, G.C. Smith, M.J. Recio, C. Reis, K. Dahm, A. Fricke, A. Krempler, A.R. Parker, S.P. Jackson, A. Gennery, P.A. Jeggo, and M. Löbrich. 2004. A pathway of double-strand break rejoining dependent upon ATM, Artemis, and proteins locating to gamma-H2AX foci. *Mol. Cell.* 16:715-724.

Rothkamm, K., and M. Löbrich. 2003. Evidence for a lack of DNA double-strand break repair in human cells exposed to very low X-ray doses. *Proc. Natl. Acad. Sci. USA.* 100:5057-5062.

Rothkamm, K., I. Krüger, L.H. Thompson, and M. Löbrich. 2003. Pathways of DNA double-strand break repair during the mammalian cell cycle. *Mol. Cell. Biol.* 23:5706-5715.

Rogakou, E.P., C. Boon, C. Redon, and W.M. Bonner. 1999. Megabase chromatin domains involved in DNA double-strand breaks in vivo. *J. Cell Biol.* 146:905-916.

Sengupta, S., A.I. Robles, S.P. Linke, N.I. Sinogeeva, R. Zhang, R. Pedeux, I.M. Ward, A. Celeste, A. Nussenzweig, J. Chen, T.D. Halazonetis, and C.C. Harris. 2004. Functional interaction between BLM helicase and 53BP1 in a Chk1-mediated pathway during S-phase arrest. *J. Cell Biol.* 166:801-813.

Shiloh, Y. 2003. ATM and related protein kinases: safeguarding genome integrity. *Nat. Rev. Cancer.* 3:155-168.

van Gent, D.C., J.H. Hoeijmakers, and R. Kanaar. 2001. Chromosomal stability and the DNA double-stranded break connection. *Nat. Rev. Genet.* 2:196-206.

Wahl, G.M., and A.M. Carr. 2001. The evolution of diverse biological responses to DNA damage: insights from yeast and p53. *Nat. Cell Biol.* 3:E277-286.

Ward, I., and J. Chen. 2004. Early events in the DNA damage response. *Curr. Top. Dev. Biol.* 63:1-35.

Zhang, X., J. Succi, Z. Feng, S. Prithivirajsingh, M.D. Story, and R.J. Legerski. 2004. Artemis is a phosphorylation target of ATM and ATR and is involved in the G2/M DNA damage checkpoint response. *Mol. Cell. Biol.* 24:9207-9220.

Zhao, B., M.J. Bower, P.J. McDevitt, H. Zhao, S.T. Davis, K.O. Johanson, S.M. Green, N.O. Concha, and B.B. Zhou. 2002. Structural basis for Chk1 inhibition by UCN-01. *J. Biol. Chem.* 277:46609-46615.

Figure 1:

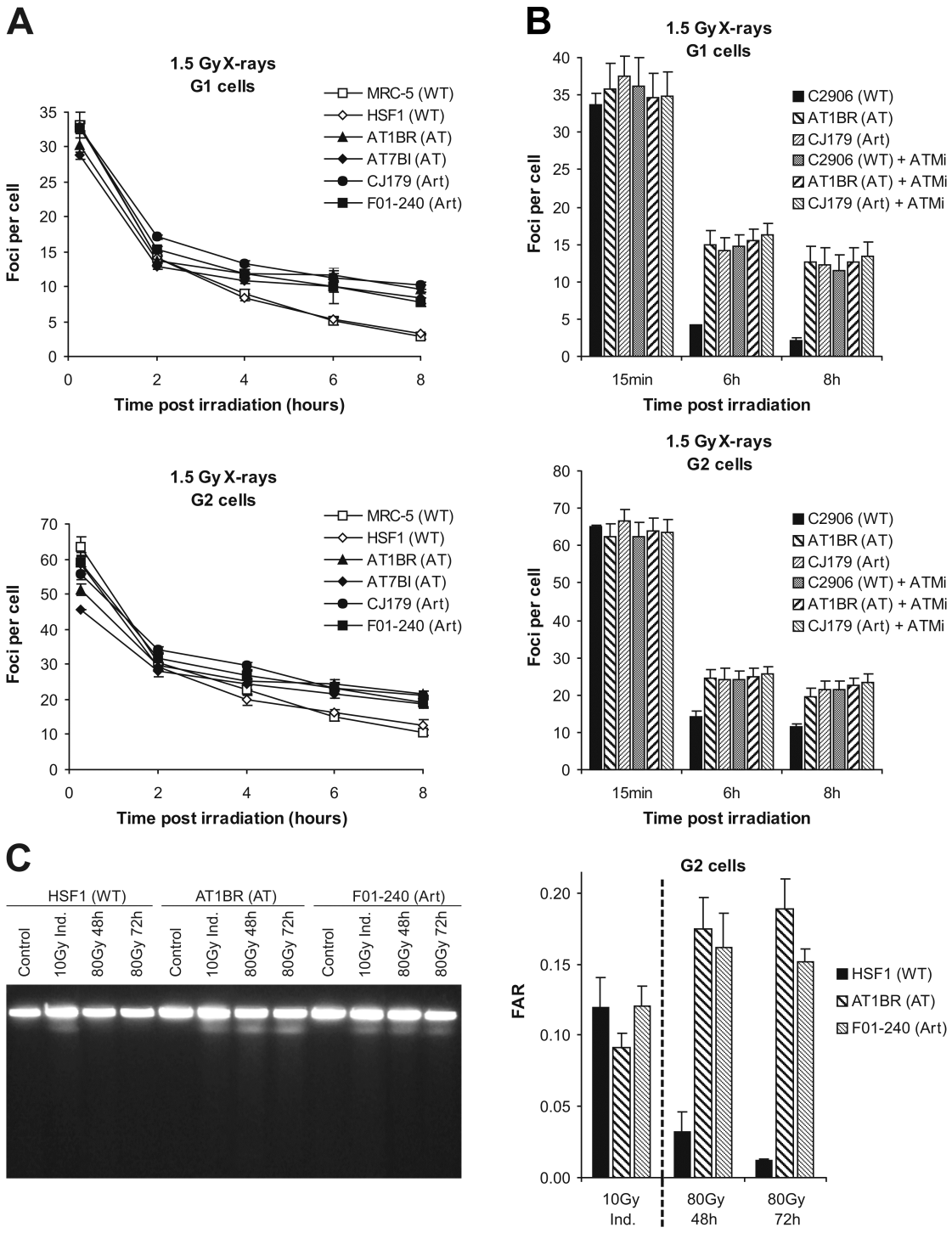

Figure 1. A-T and Artemis primary human fibroblasts exhibit a DSB repair defect in G1 and G2. (A) γH2AX foci analysis in G1- and G2-phase cells following 1.5 Gy X-irradiation. Background foci numbers were about 2 in G2 and 0.2 in G1. (B) γH2AX foci analysis in G1- and G2-phase cells following 1.5 Gy X-irradiation in the absence or presence of the ATM small molecule inhibitor KU55933 (ATMi). (C) FAR assay of [methyl-^{3}H]thymidine-labeled exponentially growing cells irradiated in G2. Left panel: Ethidium bromide-stained PFGE gel from primary human fibroblasts irradiated with 10 Gy (for assessing DSB induction) or 80 Gy (for 48 h and 72 h repair points) X-rays. Right panel: FAR values calculated from the scintillation counts of gel slices derived from PFGE gels.

Figure 2:

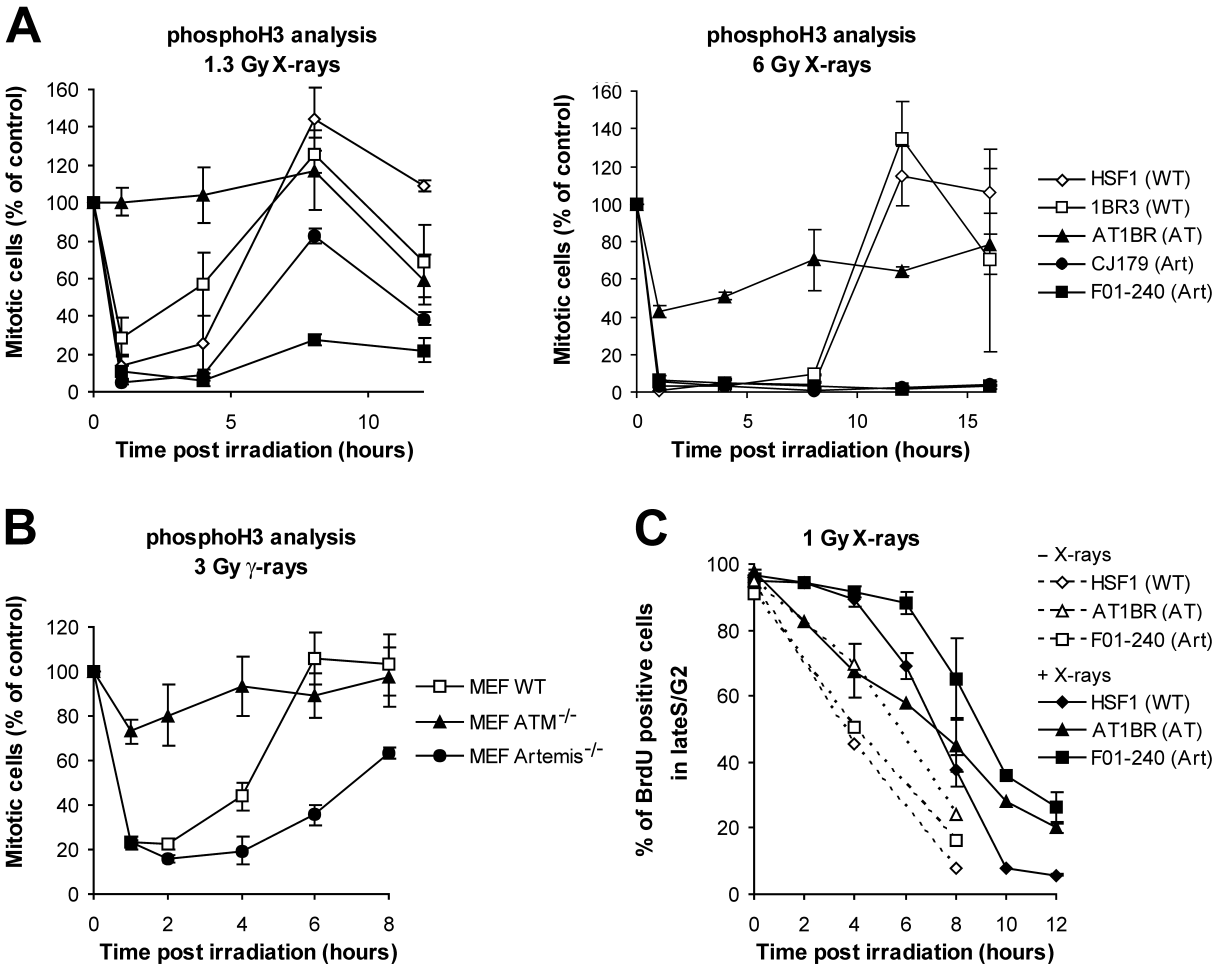

Figure 2. Artemis cells show proficient checkpoint induction and a prolonged G2/M arrest. (A) phosphoH3 analysis of primary human fibroblasts following 1.3 and 6 Gy X-irradiation. (B) phosphoH3 analysis of MEFs following 3 Gy γ-irradiation. Data shown are the percentage of mitotic cells relative to unirradiated cells at time zero. (C) FACS analysis of BrdU-labeled primary human fibroblasts. The percentage of BrdU-positive cells in late S/G2 was assessed up to 8 h after 1.5 Gy X-irradiation given at 4 h post BrdU labeling (ie when BrdU-labeled cells have progressed into late S/G2). Dotted lines represent the percentage of BrdU-positive cells in late S/G2 without irradiation.

Figure 3:

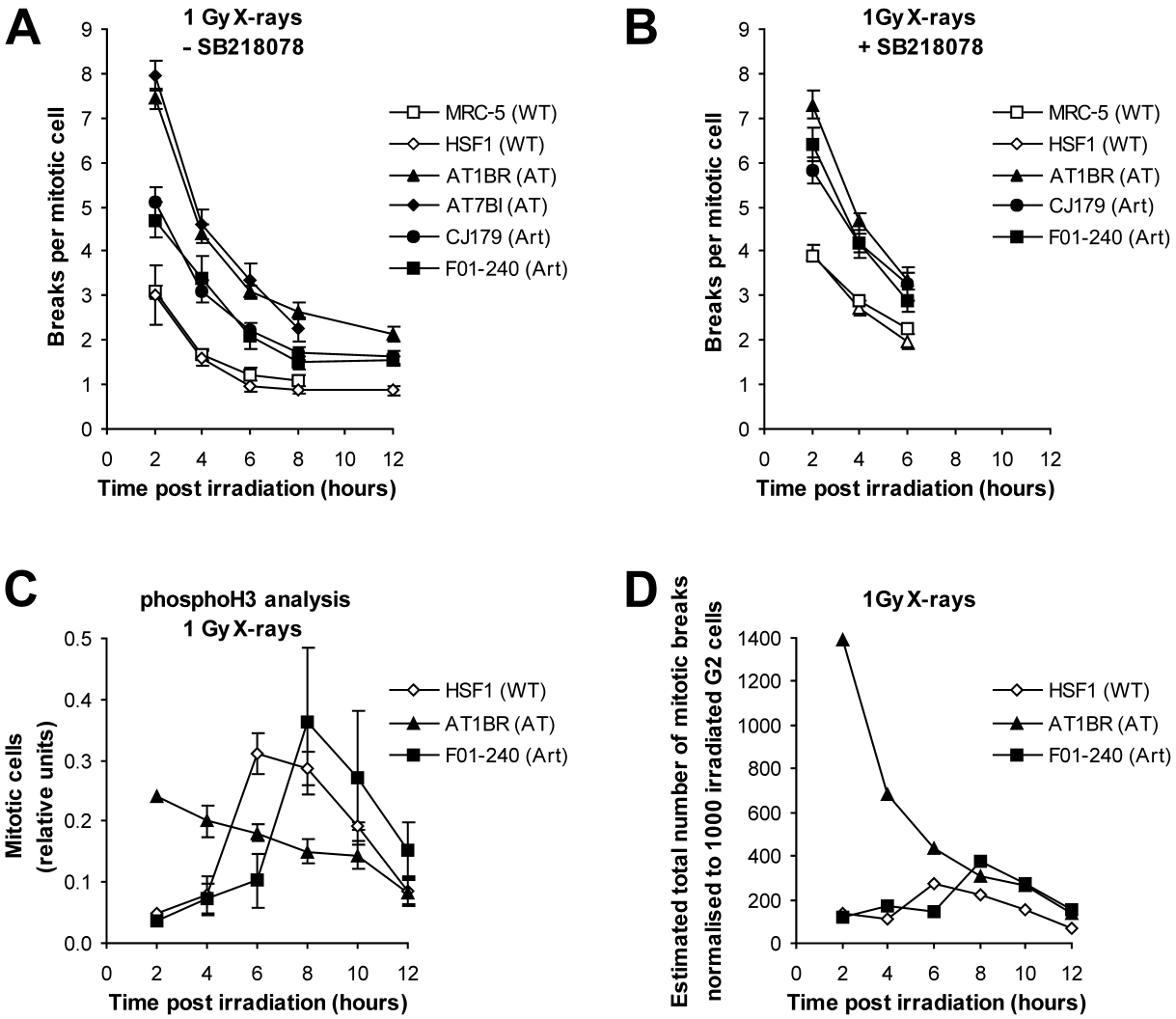

Figure 3. ATM's repair and checkpoint functions contribute to prevent chromosome breakage. (A) Chromosome breaks per mitotic cell in metaphase spreads from primary human fibroblasts harvested at varying times following 1 Gy X-irradiation in the presence of aphidicolin. Breaks in unirradiated samples were less than 0.1 and were subtracted from the breaks in the irradiated samples. (B) Same analysis as in panel A in the presence of the Chk1/2 inhibitor SB218078. SB218078 did not cause chromosome breaks in unirradiated cells. (C) phosphoH3 analysis of primary human fibroblasts after 1 Gy X-irradiation in the presence of aphidicolin (ie the same conditions used for the chromosomal analysis). The measured mitotic indices were normalised to provide the same integral value of 1 for all three cell lines. (D) Estimation of the kinetics for total mitotic chromosome breakage. The values are derived from the number of chromosome breaks per mitotic cell for cells that enter mitosis at specific time points (taken from panel A) multiplied by the number of cells reaching mitosis at these times (taken from panel C). See supplemental text for a more detailed description of panels C and D.

Figure 4:

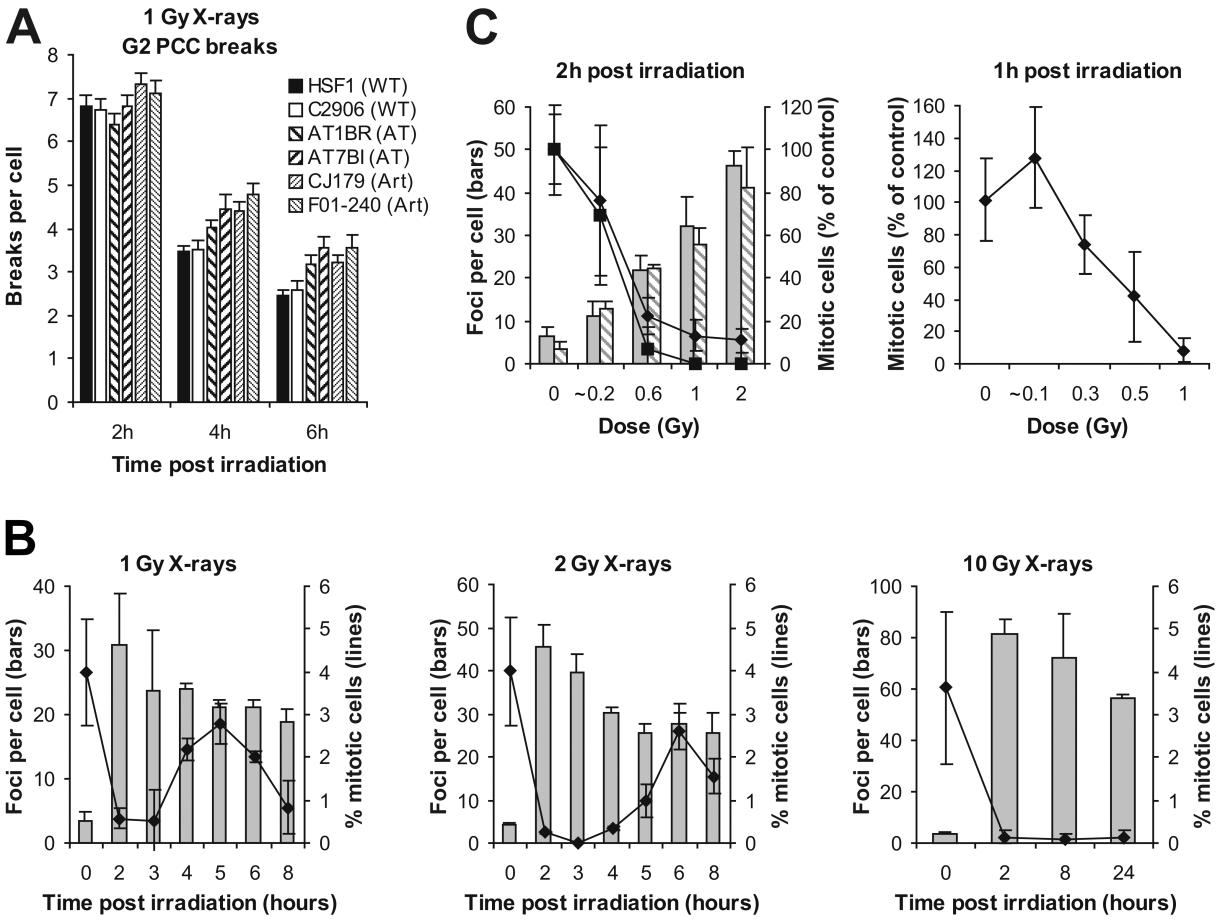

Figure 4. The G2/M checkpoint has a threshold of ~3.5 PCC breaks and ~20 γH2AX foci. (A) Analysis of G2 PCC chromosomal breaks in calyculin A-treated cells in the presence of aphidicolin at 2, 4, and 6 h after 1 Gy X-irradiation. Breaks in unirradiated samples were less than 0.2 and were subtracted from the breaks in the irradiated samples. Student's t-test was performed: $P<0.01$ for AT1BR, AT7BI, CJ179, and F01-204 compared with HSF1 or C2906 at 4 and 6 h (but not at 2 h). (B) γH2AX analysis and mitotic counting of transformed MRC-5V1 fibroblasts at varying times after 1, 2, and 10 Gy X-irradiation in the presence of aphidicolin. The analysis was done on the same samples by counting the fraction of phosphoH3 positive mitotic cells and foci numbers in CENP-F positive G2 cells, respectively. The pronounced decline in mitotic index at 8 h after 1 and 2 Gy likely reflects the depletion of G2 cells. (C) Left panel: same analysis as in panel B evaluating transformed (MRC-5V1; grey bars, diamonds) and immortalised (48BR hTert; shaded bars, squares) fibroblasts 2 h after 0, 0.2, 0.6, 1, and 2 Gy X-irradiation. Right panel: phosphoH3 analysis of primary (48BR) fibroblasts after 0, 0.1, 0.3, 0.5, and 1 Gy X-irradiation by FACS. γH2AX foci were scored on parallel samples and provided similar numbers to those of MRC-5V1 and 48BR hTert cells. Analysis was carried out 1 h post IR, since pilot experiments showed that primary cells show a more rapid onset of checkpoint arrest. Note that very short exposure times were required to deliver the low doses in these experiments, resulting in potential errors in the estimated dosimetry.

Supplemental figure legends

Suppl. Figure 1. (A) Representative immunofluorescence images of exponentially growing HSF1 cells irradiated with 1.5 Gy X-rays in the presence of aphidicolin. Treatment with aphidicolin resulted in high levels of γH2AX phosphorylation in a subset of the cells (a bright lawn-like signal as shown in the lower left panel). Double staining against γH2AX and CyclinA showed that all γH2AX-positive cells were positive for the S/G2 marker CyclinA. Double staining against γH2AX and CENP-F showed that all γH2AX-positive cells were negative for the G2 marker CENP-F. Since this γH2AX signal was observed without irradiation and was dependent on aphidicolin, we attribute it to the activation of ATR following replication arrest caused by aphidicolin. Hence, double staining against γH2AX/CENP-F allows the unequivocal identification of G1 (γH2AX and CENP-F negative), S (γH2AX positive and CENP-F negative), and G2 cells (γH2AX negative and CENP-F positive). (B) Representative FACS plots of HSF1 cells in the presence of aphidicolin following a dose of 1 Gy X-rays. Cells were BrdU labeled for 1 h, irradiated immediately after labeling and aphidicolin was added. The upper rectangles show the percentages of BrdU-positive cells in early versus late S phase. The lower rectangle indicates the percentage of BrdU-negative cells in G2. (C) γH2AX analysis in the presence or absence of aphidicolin in G2-phase MRC-5 cells. (D) γH2AX analysis in exponentially growing MEFs. The analysis was carried out in the presence of aphidicolin (similar to Fig. 1). (E) Representative FACS plots showing the percentage of BrdU-labeled primary human fibroblasts in G2 at 0, 48, and 72 h after 80 Gy X-irradiation (rectangles). Irradiation was performed 4 h after BrdU labeling.

Suppl. Figure 2. (A) G2/M checkpoint analysis by mitotic counting. The mitotic index was assessed in primary human fibroblasts at 8, 16, and 24 h after 3 and 6 Gy γ-irradiation. Nocodazole was added immediately following irradiation to accumulate cells in mitosis. (B)

Representative FACS plots of primary human fibroblasts showing mitotic cells (circles) identified by phosphoH3 staining after 1.3 and 6 Gy X-irradiation. No nocodazole was used for these experiments.

Suppl. Figure 3. (A) 53BP1 foci formation in transformed human WT fibroblasts treated with Chk1 siRNA or the Chk1 inhibitor SB218078 after exposure to 1 mM hydroxyurea for 2 h (for technical details see Stiff et al., 2006, EMBO J 25: 5775-5782). (B) phosphoH3 analysis in primary human fibroblasts at 1, 4, and 8 h after 1 Gy X-irradiation in the presence of the Chk1/2 inhibitor SB218078. (C) phosphoH3 analysis of WT MEFs at 1, 2, 4, and 6 h after 3 Gy γ-irradiation with or without SB218078. Data are shown as the percentage of mitotic cells relative to untreated and unirradiated cells at time zero. (D) γH2AX analysis in G2-phase primary human fibroblasts (HSF1) in the presence or absence of SB218078 at 2, 4, 6, and 8 h after 1.5 Gy X-irradiation. (E) Estimation of the kinetics for total mitotic chromosome breakage. The values are derived from the number of chromosome breaks per mitotic cell for cells that enter mitosis at specific time points (taken from Fig. 3A) multiplied by the number of cells reaching mitosis at these times (calculated from Fig. 2C from the decrease in the fraction of late S/G2 cells). For example: Artemis cells exhibit ~1.5 breaks per mitotic cell at 8 h post IR (Fig. 3A). Between 6 and 8 h, the fraction of BrdU-positive Artemis cells in late S/G2 decreases from ~90% to ~70%, ie ~20% of the irradiated G2 cells have entered mitosis between 6 and 8 h (Fig. 2C). Thus, we multiplied the value of 1.5 by 0.2 (to account for the fraction of G2 cells entering mitosis) and by 1000 (to normalise it to 1000 irradiated G2 cells). Thus, we obtained a value of ~300 total mitotic breaks for Artemis cells in the time window 6-8 h. This number means that 1000 irradiated G2-phase Artemis cells give rise to ~300 mitotic breaks in the time period between 6 and 8 h post IR with 1 Gy (the 12-h data points in Fig. 3A were taken to calculate total break numbers in the time windows 8-10 h and 10-12 h). (F) γH2AX analysis in mitotic human fibroblasts (hTert WT cells) at 6 h

after 1 Gy X-irradiation. The analysis was carried out in the presence of aphidicolin under checkpoint-proficient conditions (ie without SB218078). The phosphoH3 positive cells represent cells in different stages of mitosis. The average foci number in phosphoH3 positive cells at the 6 h time point was 12, similar to the foci number of 14 obtained in a parallel sample from the analysis of CENP-F positive G2 cells.

Supplemental text

Estimation of the kinetics for total chromosome breakage

Fig. 3D aims to compare the time course for total mitotic chromosome breakage for three different cell lines; A-T, Artemis and WT. We have measured for all three lines the mitotic index at defined times post irradiation by phosphoH3 FACS analysis under the same conditions used for the chromosomal analysis, ie in the presence of aphidicolin (Fig. 3C). However, different cell lines can vary considerably in their fraction of G2 phase cells. Moreover, the majority but not all G2-irradiated cells leave G2 within 12 h with slight differences between the three cell lines (see Fig. 2C). We have considered the first variation (different G2 proportions) by normalising the phosphoH3 data in Fig. 3C such that the sum of the mitotic indices measured up to 12 h post irradiation is the same for all three cell lines and the second variation by multiplying these mitotic indices with the measured proportion of G2-irradiated cells that leave G2 within 12 h. The latter values are derived from Fig. 2C. For example: Artemis cells entering mitosis at 8 h post IR exhibit ~1.5 breaks per mitotic cell (Fig. 3A). At this time, the relative mitotic index for Artemis cells is about 0.35. Thus, we multiplied the value of 1.5 by 1000 (to normalise it to 1000 irradiated G2 cells), then by 0.75 (because 75% of all irradiated G2 Artemis cells leave G2 within 12 h, see Fig. 2C), and finally by 0.35 (because 35% of all cells that leave G2 within 12 h do this at the 8 h time point). This provides a value of ~400 mitotic breaks for Artemis cells at 8 h (Fig. 3D).

Suppl. Figure 1:

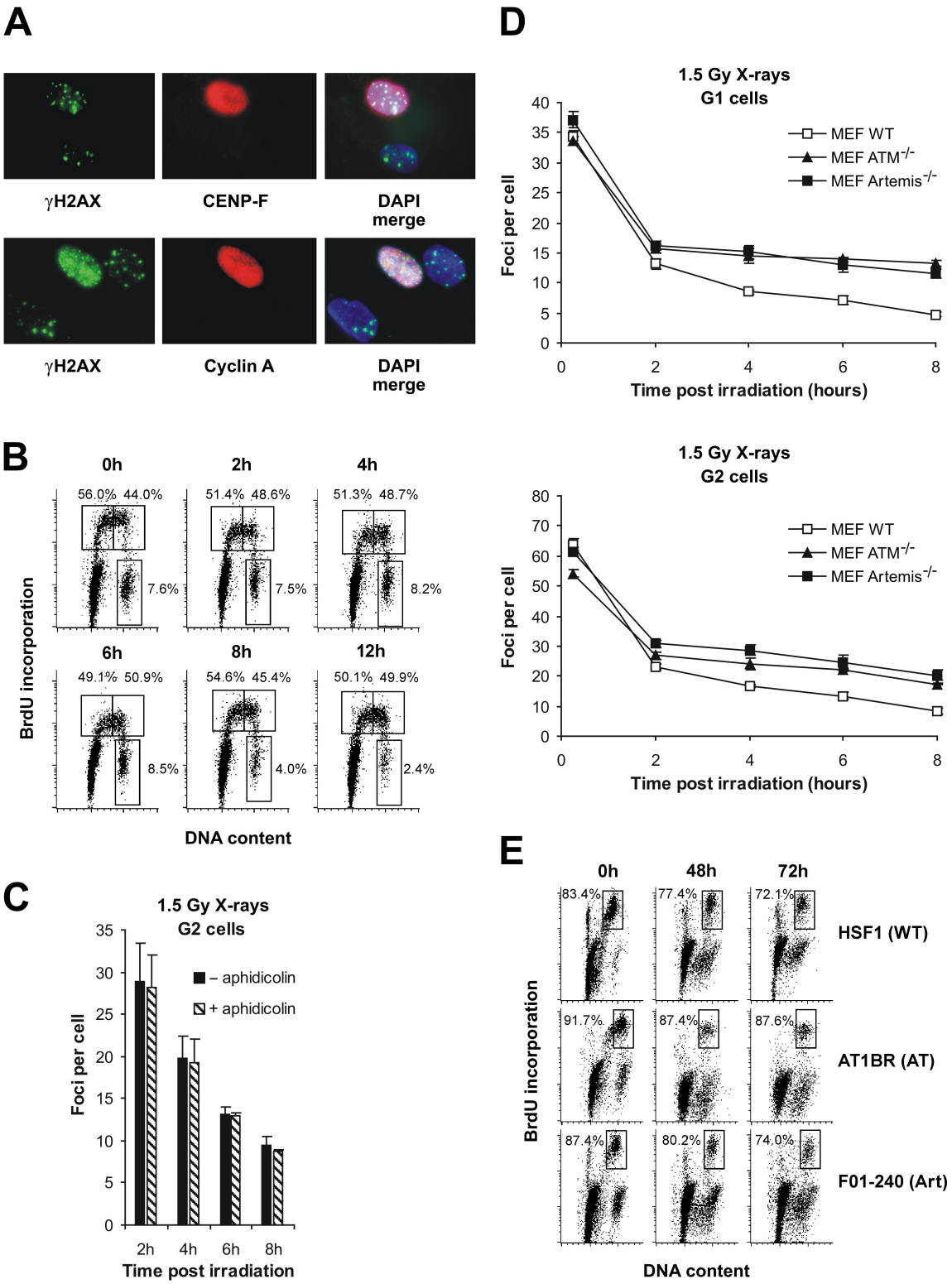

Suppl. Figure 2:

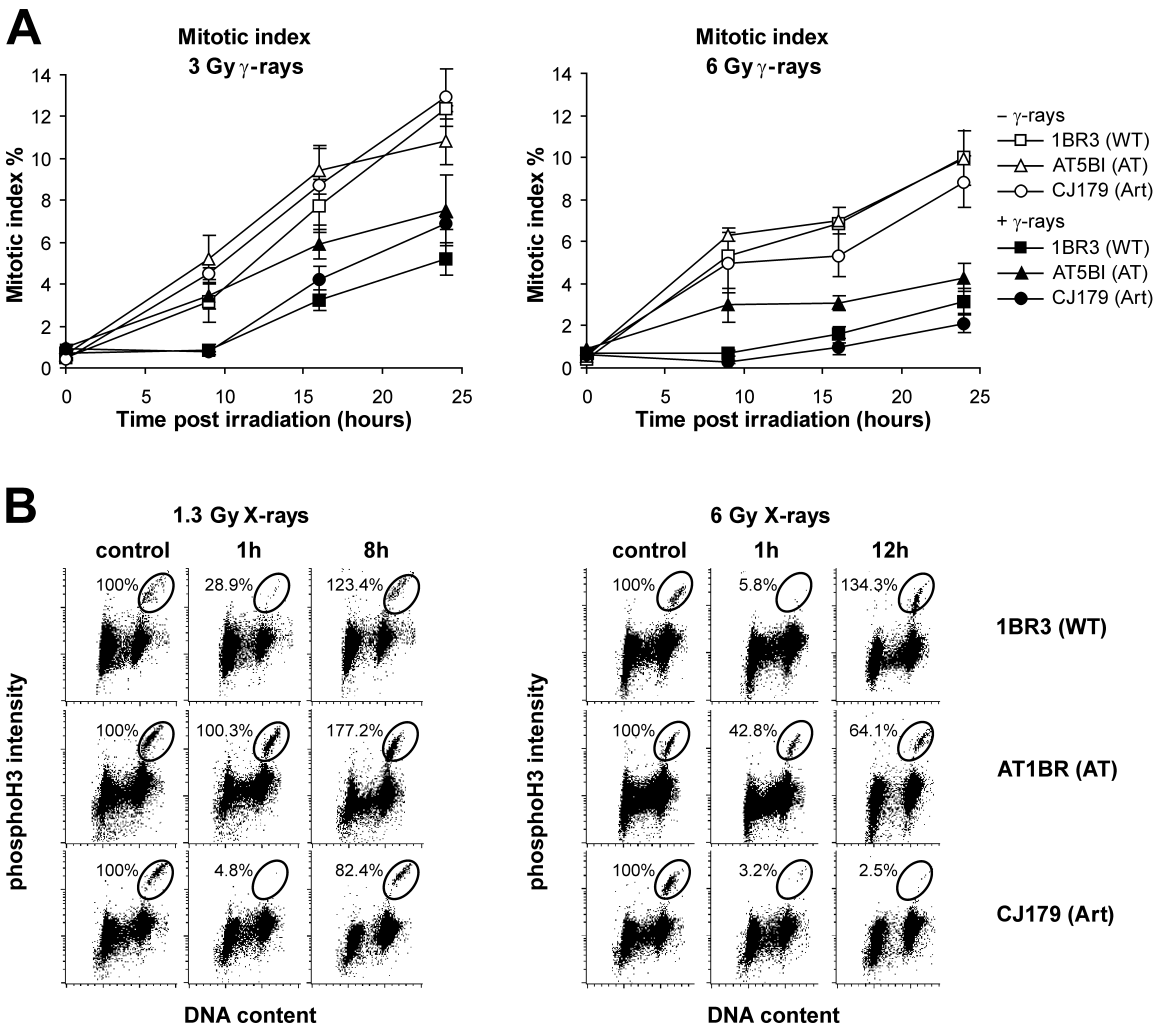

Suppl. Figure 3: